Bioorganic & Medicinal Chemistry 18 (2010) 4310–4316

Contents lists available at ScienceDirect

Bioorganic & Medicinal Chemistry

journal homepage: www.elsevier.com/locate/bmc

Synthesis, molecular modeling and biological evaluation of dithiocarbamates as novel antitubulin agents

Yong Qian, Gao-Yuan Ma, Ying Yang, Kui Cheng, Qing-Zhong Zheng, Wen-Jun Mao, Lei Shi, Jing Zhao *, Hai-Liang Zhu *

State Key Laboratory of Pharmaceutical Biotechnology, Nanjing University, Nanjing 210093, People's Republic of China

ARTICLE INFO

Article history:
Received 23 February 2010
Revised 24 April 2010
Accepted 27 April 2010
Available online 20 May 2010

Keywords:
Dithiocarbmate
Chalcone
Molecular modeling
Antitubulin polymerization

ABSTRACT

A series of novel dithiocarbamate compounds with the chalcone scaffold have been designed and synthesized, and their biological activities were also evaluated as potential antiproliferation and antitubulin polymerization inhibitors. Compound **2n** showed the most potent biological activity in vitro, which inhibited the growth of MCF-7 cells with IC_{50} of 0.04 ± 0.01 μM and the polymerization of tubulin with IC_{50} of 6.8 ± 0.6 μM. To understand the tubulin–inhibitor interaction and the selectivity of the most active compound towards tubulin, molecular modeling studies were performed to dock compound **2n** into the colchicine binding site, which suggested probable inhibition mechanism.

1. Introduction

Microtubules are key cytoskeletal filaments and are involved in numerous cellular functions, including cell motility, vesicle transport and cell division. Microtubules are in dynamic equilibrium with tubulin dimers.[1] Disruption of the dynamic equilibrium will lead to cell cycle arrest or cell apoptosis. Given their significant role in the growth and function of cells, microtubules are among the most important molecular targets for cancer chemotherapeutic agents.

Recently a number of small molecules were discovered to bind to tubulins, interfering with the polymerization or depolymerization of microtubules and then inducing cell cycle arrest, resulting in cell death.[2–5] Fore example, Combretastatin A-4 (CSA-4), which was isolated from the South African tree *combretum cattrum*, was found to inhibit the polymerization of tubulin by binding to the colchicine site.[6,7] Colchicine is the first drug that is well known to bind tubulin, and the colchicine binding site has been characterized recently.[8] The development of ketones as tubulin binding agents such as chalcones was reviewed.[9]

Chalcones (1,3-diarylpropenones) are an important pharmacophore of natural products and the synthetic precursors to various flavonoids and isoflavonoids. A variety of pharmacological activities of chalcones have been reported, including anticancer, anti-inflammatory, immunomodulatory, antibacterial, immunosuppressive, antiprotozoan activity, antimalarial,[10–16] antimitotic, and antiproliferative.[3,11,12,17–19]

On the other hand, dithiocarbamate (DTC) derivatives are well known as rubber additives, vulcanizing agents, fungicides,[20] antimicrobial agents,[21] antitumor drugs,[22] and prophylactic or therapeutic agents for metal toxicity.[23–25] Recently, Yang et al. have described a series of chromone derivatives bearing dithiocarbamate moieties which displayed apoptosis-inducing effects on tumor cell lines.[26]

Herein we report the synthesis and bioactivities of a series of new substituted dithiocarbamate compounds based on intermediate chalcones. Their antiproliferative and inhibition of tubulin polymerization activities were evaluated. Molecular modeling studies were consequently performed to understand tubulin–inhibitor interaction. The docking results confirmed that the combination of static and hydrophobic interactions and hydrogen bonding may contribute to the potent biological activities.

2. Results and discussion

2.1. Chemistry

The synthesis of compounds **2a**–**2t** is outlined in Scheme 1. First, a series of chalcones were prepared by the Claisen–Schmidt condensation between ketones and aldehydes in the presence of KOH in MeOH in 80–85% yield.[11] The desired dithiocarbamates **2a**–**2t** could be obtained by one-pot reaction of diethylamine, carbon disulfide and intermediate chalcones (yield: 85–90%).[27]

* Corresponding authors. Tel.: +86 25 8359 2572; fax: +86 25 8359 2672 (H.-L.Z.).
E-mail address: zhuhl@nju.edu.cn (H.-L. Zhu).

0968-0896/$ - see front matter © 2010 Elsevier Ltd. All rights reserved.
doi:10.1016/j.bmc.2010.04.091

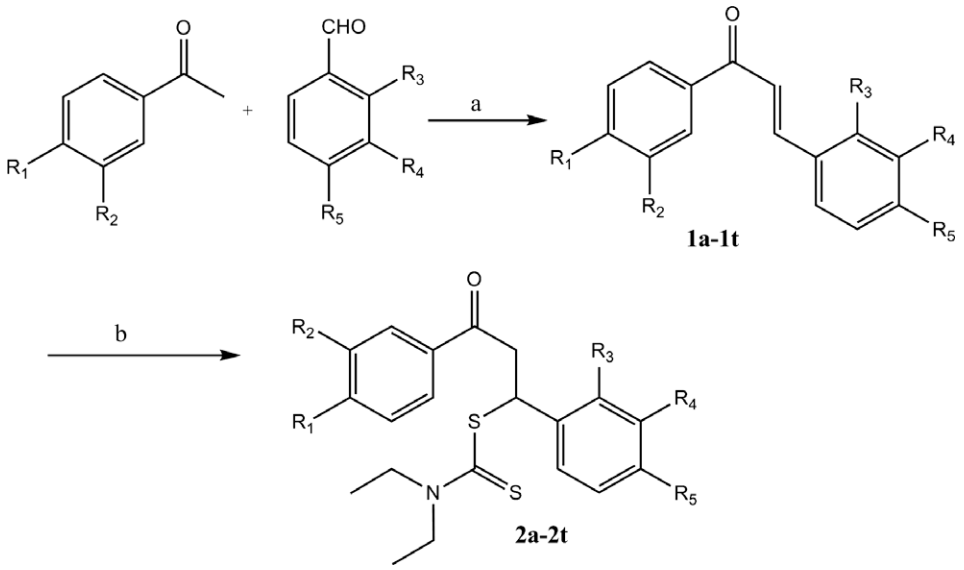

Scheme 1. Synthesis of dithiocarbamates **2a–2t**. Reagents and conditions: (a) KOH, M_eOH, rt; (b) CS_2, dithylamine, CH_2Cl_2.

(Table 1) All the target compounds were characterized by ^1H NMR, Elemental analysis, and mass spectrum. Furthermore, the crystal structure of compound **2l** was determined by single crystal X-ray diffraction analysis in Figure 1.

2.2. Bioactivity

All synthesized dithiocarbamate compounds **2a–2t** were evaluated for their ability to antiproliferative activities against MCF-7 human breast carcinoma cells. The results were summarized in Table 2. A number of dithiocarbamate compounds bearing the same dithiocarbamate (DTC) moiety showed remarkable effects on antiproliferative activities. The compounds with para halogen substituted (**2d**, **2e**, **2f**) exhibited significant antiproliferative activity and the potency order is F < Cl < Br. The results demonstrated that a hydrophobic and electron-withdrawing halogen group may have slightly improved antiproliferative activity and other electron-donating substituted (**2b**, **2c**) had minimal effects relative to those of **2d**. Compounds (**2d**, **2e**) with *p*-substituted group showed slightly more potent activities than those of *o*-substituted (**2g**, **2h**) and m-substituted (**2i**). Compound **2j** in which A-ring was substituted by methyl group showed poor activity, suggesting that aromaticity of the A-ring was critical for the potent activity. Compounds (**2n**, **2k**, **2m**) with chloro-substitution or methoxy-substitution showed stronger antitumor activity compared to compound with a *p*-bromo group substituted in the A ring such as **2l**, suggesting that the enhancing order of the substituent on A-ring is: 4-Br < 4-OMe = 3, 4-Cl < 4-Cl. Interestingly, a similar phenomenon was also observed with substituents of *p*-Br (**2o**) and *p*-OMe (**2q**) on A-ring, having the same *p*-OMe substituent on B-ring, and showed IC_{50} values of 5 ± 0.6 and 0.8 ± 0.05 μM, respectively. Compound **2s**, with a *p*-OMe group in the A-ring and an *o*-Cl group in the B-ring, revealed the similar activity to **2n** containing *p*-Cl

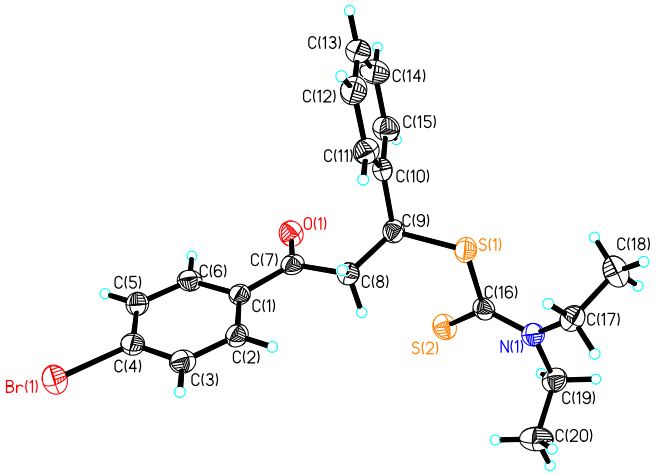

Figure 1. Crystal structure diagrams of compound **2l**. Molecule structure diagram with displacement ellipsoids being at the 30% probability level and H atoms are shown as small spheres of arbitrary radii.

Table 1
Structure of dithiocarbamates **2a–2t**

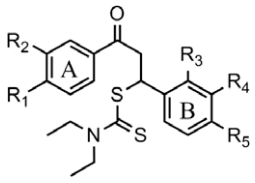

Compound	R1	R2	R3	R4	R5
2a	H	H	H	H	H
2b	H	H	H	H	OMe
2c	H	H	H	H	Me
2d	H	H	H	H	Br
2e	H	H	H	H	Cl
2f	H	H	H	H	F
2g	H	H	OMe	H	H
2h	H	H	Cl	H	H
2i	H	H	H	NO_2	H
2j	A=CH_3		H	H	H
2k	OMe	H	H	H	H
2l	Br	H	H	H	H
2m	Cl	Cl	H	H	H
2n	Cl	H	H	H	H
2o	Br	H	H	H	OMe
2p	Br	H	H	H	F
2q	OMe	H	H	H	OMe
2r	OMe	H	H	H	Me
2s	OMe	H	Cl	H	H
2t	OMe	H	H	H	Cl

Table 2
Inhibition of tubulin polymerizaton and inhibition (IC_{50}) of MCF-7 cells proliferation by compound **2a–2t**

Compound	MCF-7[a] IC_{50} ± SD (μM)	Tubulin[b] IC_{50} ± SD (μM)
2a	17 ± 3	130 ± 40
2b	4.6 ± 0.3	45 ± 2
2c	20 ± 8	220 ± 10
2d	0.08 ± 0.03	12 ± 4
2e	0.12 ± 0.02	15 ± 3
2f	0.7 ± 0.08	80 ± 7
2g	16 ± 4	150 ± 14
2h	4.5 ± 0.12	52 ± 5
2i	9 ± 0.7	90 ± 8
2j	23 ± 3	250 ± 20
2k	4.5 ± 0.7	62 ± 40
2l	5 ± 0.15	65 ± 15
2m	4.5 ± 0.2	60 ± 10
2n	0.04 ± 0.01	6.8 ± 0.6
2o	5 ± 0.6	52 ± 7
2p	1 ± 0.25	18 ± 4
2q	0.8 ± 0.05	84 ± 6
2r	17 ± 4	180 ± 20
2s	0.07 ± 0.01	10 ± 2
2t	16 ± 4	140 ± 30
Colchicine	0.017 ± 0.01	3.2 ± 0.4
CSA-4	0.013 ± 0.003	2.2 ± 0.2

[a] Inhibition the growth of MCF-7 human breast carcinoma cells.
[b] Inhibition of tubulin polymerization.

substituent on A-ring. However, compound **2t** displayed a poor activity.

To examine whether the compounds interact with tubulin and inhibit tubulin polymerization in vitro, we performed the tubulin assembly assay. As shown in Table 2, compounds **2d**, **2e**, **2n**, **2s** showed strong inhibitory effect and their 50% tubulin polymerization inhibition about 12 ± 4 μM, 15 ± 3 μM, 6.8 ± 0.6 μM, 10 ± 2 μM, respectively. Compound **2n** displayed the most potent anti-tubulin polymerization activity (Table 2). The result confirmed that the antiproliferative effect was mediated by direct interaction of compounds with tubulin.

Compound **2n** was also performed cell cycle analysis using flow cytometry. Cell cycle analysis (Fig. 3) showed that the compound **2n** strongly induced G2/M arrest in MCF-7 cells, and the effect was observed in a dose-independent manner after treatment for 24 h increasing amounts of the compound. About 39.5% of the cells were arrested in the G2/M phase after treatment with 250 nm **2n** for 24 h. These findings indicated a continuing impairment of cell division and confirmed compound **2n** was a potent antitubulin agent.

To gain more understanding on compound **2n**'s potency, we proceeded to examine the interaction of the compound **2n** with tubulin (PDB code: 1SA0). The molecular docking was performed by simulation of compound **2n** in the colchicine binding site of tubulin. All docking runs were applied the Lamarckian genetic algorithm of Auto-Dock 4.0.[28] The calculated free energies of binding were used as the parameter for the selection of the cluster of docking posed to be evaluated, in which the binding mode of the lowest energy structure located in the top docking cluster. The selected pose of **2n** had an estimated free energy of binding of −10.76 kcal/mol (free energy of binding of control compounds colchicine and CSA-4 is −8.86 kcal/mol and −7.62 kcal/mol, respectively). The structure of lowest energy in the top docking cluster was showed in Figure 2A. The docking results demonstrated that **2n** interacted with the colchicine binding site of tubulin via hydrophobic interactions and binding is stabilized by one hydrogen bond (SER178: angle O···H–O = 168.022°, distance = 2.111 Å). These residues (CYS241, SER178) were also found to be involved in the binding of other tubulin binding agents.[29] As depicted in Figure 2B, a, c and d depicted the 3D model of the interaction between **2n**, colchicine, CSA-4 and the colchicine binding site. Comparing this model, the hydrophobic pockets of colchicine binding site were occupied by compounds, and the difference was the arrangement on the enzyme surface. In particular, **b** depicted the molecular surface model of compound **2n** interaction with the site, showing well binding affinity to the target. In the **2n** binding model, more details revealed that there are some key roles of the interaction of **2n** and tubulin (Fig. 2A). The chlorophenyl moiety of A-ring occupied a pocket bounded by ALA180, LEU255, and LYS352. It should be noted that the static interaction between Cl group and LYS352 might play a role. The phenyl moiety of B ring was embedded in a hydrophobic pocket constructed by the side chains of residues of CYS241, LEU248 and LEU255. Moreover, the binding of compound **2n** to tubulin was stabilized by hydrogen bond with SER178. Overall, the results suggested that **2n** interacted well with tubulin, similar to colchicine and CSA-4.[3,30,31]

3. Conclusion

In the present work, we synthesized and evaluated a series of novel antitubulin polymerization inhibitors containing a dithiocarbamate moiety. These chalcone-type compounds exhibited potent tubulin polymerization inhibitory activity and antiproliferative activity against MCF-7 human breast carcinoma cells. Compound **2n** demonstrated the most potent activity which inhibited the growth of MCF-7 cells with IC_{50} of 0.04 ± 0.01 μM and inhibited

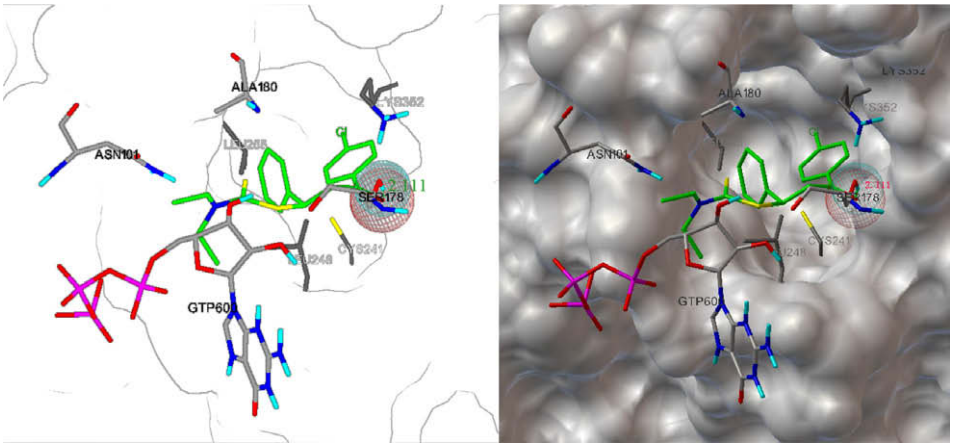

Figure 2A. compound **2n** (carbon atom are green) docked into the tubulin pocket. Both side chains of important active site amino acids and hydrogen bonds are shown: Ser-178 (angle O···H–O = 168.022°, distance = 2.111 Å).

the polymerization of tubulin with IC_{50} of 6.8 ± 0.6 μM (control compound CSA-4, showed antiproliferation activity against MCF-7 cells (IC_{50} = 0.013 ± 0.003 μM) and antitubulin polymerization activity (IC_{50} = 2.2 ± 0.2 μM), respectively). Molecular docking

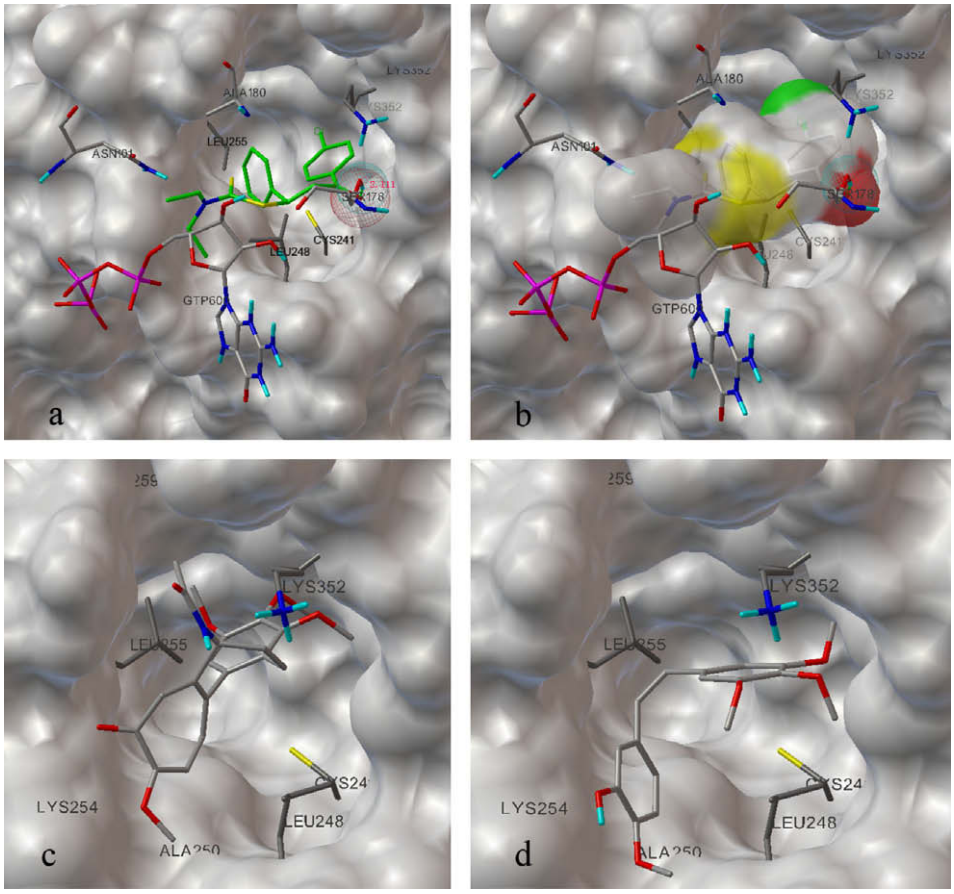

Figure 2B. Comparison of colchicine, CSA-4 and compounds **2n** binding model with tubulin complex. (a) 3D model of the interaction between compound **2n** and the colchicine binding site. The protein is represented by molecular surface. **2n** is depicted by sticks and balls. (b) 3D model of interaction between compound **2n** and the colchicine binding site. The protein is represented by molecular surface. **2n** is depicted by molecular surface and sticks and balls. (c) 3D model of the interaction between colchicine and the colchicine binding site. The protein is represented by molecular surface. colchicine is depicted by sticks and balls. (d) 3D model of the interaction between CSA-4 and the colchicine binding site. The protein is represented by molecular surface. CSA-4 is depicted by sticks and balls.

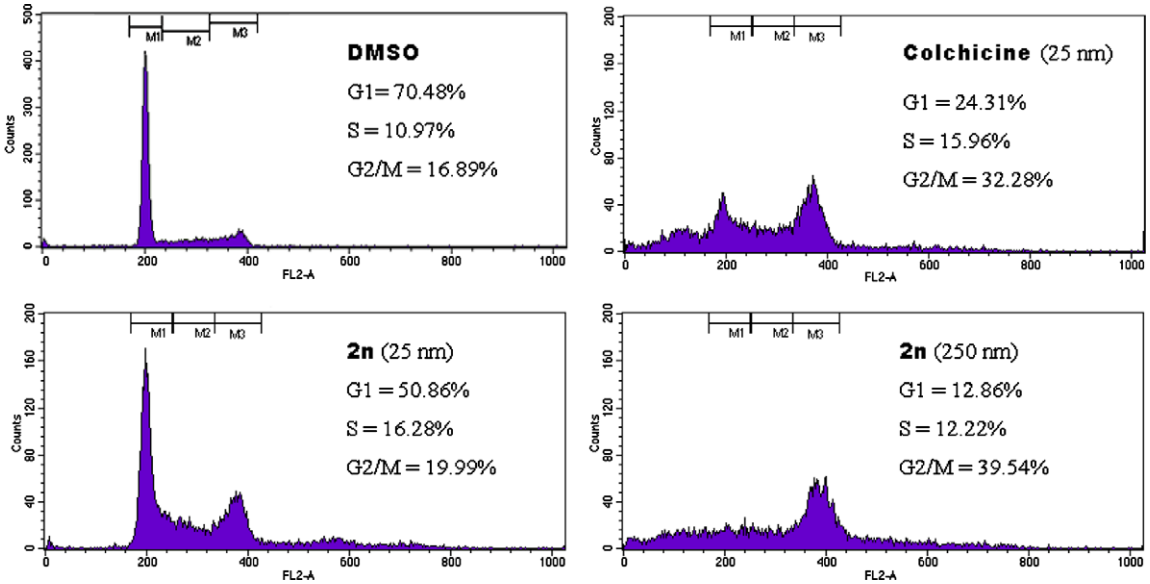

Figure 3. Cell cycle analysis of MCF-7 cells treated with compound **2n** using flow cytometry. Cells were harvested after treatment with **2n** for 24 h and subjected to cell cycle analysis. The percentage of cells in each cell cycle phase was indicated.

was performed to study the inhibitor–tubulin protein interactions. Analysis of the compound **2n**'s binding conformation in the colchicine binding site demonstrated that a combination of several interactions with the protein residues led to the antitubulin polymerization and cytotoxicity. We are presently plan to utilize the molecular modeling studies to design and synthesize more potent tubulin polymerization inhibitors.

4. Experiments

4.1. Materials and measurements

All chemicals and reagents used in current study were of analytical grade. All the ^{1}H NMR spectra were recorded on a Bruker DRX 500 or DPX 300 model Spectrometer in $CDCl_3$ and chemical shifts was reported in ppm (δ). ESI-MS spectra were recorded on a Mariner System 5304 Mass spectrometer. Elemental analyses were performed on a CHN-O-Rapid instrument. TLC was performed on the glass-backed silica gel sheets (Silica Gel 60 Å GF254) and visualized in UV light (254 nm). Column chromatography was performed using silica gel (200–300 mesh) eluting with ethyl acetate and petroleum ether.

4.2. General procedure for synthesis of chalcones

To a stirred solution of acetophenone derivatives or acetone (1 mmol) and a benzaldehyde derivatives (1 mmol) in MeOH (30 mL) was added 6 M KOH (4 mL) and the reaction mixture was stirred until the solids formed. The products were filtrated and washed carefully with ice water and cool MeOH; the resulting chalcones were purified by crystallization from MeOH in refrigerator.

4.3. General procedure for the preparation of dithiocarbamates

The CS_2 (2.5 mmol) and chalcones (2 mmol) were dissolved in CH_2Cl_2 (2 mL) and the solution was cooled to 0 °C in an ice bath.[27] Amine (2.25 mmol) was slowly added and the reaction mixture was stirred at 0 °C for 30 min. Then, the solution was warmed to room temperature and stirred for another 24 h. After the end of the reaction, the solvents were removed in vacuum and the residue was purified by column chromatography on silica gel (ethyl acetate–petroleum ether, 1/10–1/20) affording the compound dithiocarbamates (**2a**–**2t**). (Scheme 1).

4.3.1. 3-Oxo-1,3-diphenylpropyl diethylcarbamodithioate (2a)

^{1}H NMR (300 MHz, $CDCl_3$): δ 1.24–1.29 (m, 6H); 3.67–4.19 (m, 6H); 6.08–6.13 (dd, J = 4.7, 9.7 Hz, 1H); 7.13–7.21 (m, 2H); 7.32–7.56 (m, 6H); 7.96–8.00 (m, 2H). ESI-MS: 358.1 ($C_{20}H_{23}NOS_2$, $[M+H]^+$). Anal. Calcd for $C_{20}H_{23}NOS_2$: C, 67.19; H, 6.48; N, 3.92. Found: C, 67.58; H, 6.61; N, 4.28.

4.3.2. 1-(4-Methoxyphenyl)-3-oxo-3-phenylpropyl diethylcarbamodithioate (2b)

^{1}H NMR (300 MHz, $CDCl_3$): δ 1.26–1.27 (m, 6H); 3.65–3.74 (m, 3H); 3.76 (s, 3H); 4.01–4.19 (m, 3H); 5.62–5.67 (dd, J = 4.2, 10.4 Hz, 1H); 6.80–6.83 (m, 2H); 7.32–7.35 (m, 2H); 7.40–7.45 (m, 2H); 7.51–7.56 (m, 1H); 7.97–8.00 (m, 2H). ESI-MS: 388.1 ($C_{21}H_{26}NO_2S_2$, $[M+H]^+$). Anal. Calcd for $C_{21}H_{25}NO_2S_2$: C, 65.08; H, 6.50; N, 3.61. Found: C, 65.44; H, 6.72; N, 3.94.

4.3.3. 3-Oxo-3-phenyl-1-p-tolylpropyl diethylcarbamodithioate (2c)

^{1}H NMR (300 MHz, $CDCl_3$): δ 1.22–1.34 (m, 6H); 2.88 (s, 3H); 3.67–4.17 (m, 6H); 5.63–5.68 (dd, J = 4.2, 10.2 Hz, 1H); 7.08 (d, J = 7.68 Hz, 2H); 7.30 (d, J = 8.04 Hz, 2H); 7.38–7.43 (m, 2H); 7.49–7.54 (m, 1H); 7.95–7.99 (m, 2H). ESI-MS: 392.1 ($C_{21}H_{26}NOS_2$, $[M+H]^+$). Anal. Calcd for $C_{21}H_{25}NOS_2$: C, 67.88; H, 6.78; N, 3.77. Found: C, 68.12; H, 6.98; N, 4.08.

4.3.4. 1-(4-Bromophenyl)-3-oxo-3-phenylpropyl diethylcarbamodithioate (2d)

^{1}H NMR (300 MHz, $CDCl_3$): δ 1.25–1.33 (m, 6H); 3.66–4.08 (m, 6H); 5.67–5.72 (dd, J = 4.2, 9.9 Hz, 1H); 7.30–7.33 (m, 2H); 7.40–7.47 (m, 4H); 7.53–7.58 (m, 1H); 7.95–7.97 (m, 2H). ESI-MS: 436.0 ($C_{20}H_{23}BrNOS_2$, $[M+H]^+$). Anal. Calcd for $C_{20}H_{22}BrNOS_2$: C, 55.04; H, 5.08; N, 3.21. Found: C, 55.37; H, 5.27; N, 3.43.

4.3.5. 1-(4-Chlorophenyl)-3-oxo-3-phenylpropyl diethylcarbamodithioate (2e)

^{1}H NMR (300 MHz, $CDCl_3$): δ 1.23–1.29 (m, 6H); 3.68–4.03 (m, 6H); 5.67–5.72 (dd, J = 4.3, 10.0 Hz, 1H); 7.23 (s, 1H); 7.35–7.59 (m, 6H); 7.94–8.00 (m, 2H). ESI-MS: 392.1 ($C_{20}H_{23}ClNOS_2$, $[M+H]^+$). Anal. Calcd for $C_{20}H_{22}ClNOS_2$: C, 61.28; H, 5.66; N, 3.57. Found: C, 61.55; H, 5.87; N, 3.86.

4.3.6. 1-(4-Fluorophenyl)-3-oxo-3-phenylpropyl diethylcarbamodithioate (2f)

^{1}H NMR (300 MHz, $CDCl_3$): δ 1.26–1.28 (m, 6H); 3.65–4.09 (m, 6H); 5.67–5.72 (dd, J = 4.4, 10.2 Hz, 1H); 6.93–6.99 (t, J = 8.61 Hz, 2H); 7.37–7.56 (m, 5H); 7.94–7.97 (m, 2H). ESI-MS: 376.1 ($C_{20}H_{23}FNOS_2$, $[M+H]^+$). Anal. Calcd for $C_{20}H_{22}FNOS_2$: C, 63.97; H, 5.91; N, 3.73. Found: C, 64.33; H, 6.13; N, 3.99.

4.3.7. 1-(2-Methoxyphenyl)-3-oxo-3-phenylpropyl diethylcarbamodithioate (2g)

^{1}H NMR (300 MHz, $CDCl_3$): δ 1.16–1.20 (m, 6H); 3.62–4.08 (m, 6H); 3.74 (s, 3H); 5.91–5.96 (dd, J = 4.7, 9.9 Hz, 1H); 6.75–6.82 (m, 2H); 7.09–7.18 (m, 1H); 7.31–7.46 (m, 4H); 7.89–7.92 (m, 2H). ESI-MS: 388.1 ($C_{21}H_{26}NO_2S_2$, $[M+H]^+$). Anal. Calcd for $C_{21}H_{25}NO_2S_2$: C, 65.08; H, 6.50; N, 3.61. Found: C, 65.39, H, 6.72; N, 3.92.

4.3.8. 1-(2-Chlorophenyl)-3-oxo-3-phenylpropyl diethylcarbamodithioate (2h)

^{1}H NMR (300 MHz, $CDCl_3$): δ 1.24–1.29 (m, 6H); 3.66–4.03 (m, 6H); 5.69–5.73 (dd, J = 4.3, 10.0 Hz, 1H); 7.19–7.56 (m, 7H); 7.95–7.98 (m, 2H). ESI-MS: 392.1 ($C_{20}H_{23}ClNOS_2$, $[M+H]^+$). Anal. Calcd for $C_{20}H_{22}ClNOS_2$: C, 61.28; H, 5.66; N, 3.57. Found: C, 61.57; H, 5.86; N, 3.87.

4.3.9. 1-(3-Nitrophenyl)-3-oxo-3-phenylpropyl diethylcarbamodithioate (2i)

^{1}H NMR (300 MHz, $CDCl_3$): δ 1.23–1.29 (m, 6H); 3.64–3.92 (m, 6H); 5.68–5.72 (dd, J = 4.4, 10.2 Hz, 1H); 7.43–7.88 (m, 7H); 7.98–8.12 (m, 2H). ESI-MS: 403.1 ($C_{21}H_{22}N_2O_3S_2$, $[M+H]^+$). Anal. Calcd for $C_{21}H_{21}N_2O_3S_2$: C, 59.68; H, 5.51; N, 6.96. Found: C, 59.93; H, 5.66; N, 7.28.

4.3.10. 3-Oxo-1-phenylbutyl diethylcarbamodithioate (2j)

^{1}H NMR (300 MHz, $CDCl_3$): δ 1.22–1.28 (m, 6H); 2.14 (s, 3H); 3.61–4.24 (m, 6H); 5.61–5.67 (m, 1H); 7.18–7.42 (m, 3H); 7.38–7.51 (m, 2H). ESI-MS: 296.1 ($C_{15}H_{22}NOS_2$, $[M+H]^+$). Anal. Calcd for $C_{15}H_{21}NOS_2$: C, 60.98; H, 7.16; N, 4.74. Found: C, 61.33; H, 7.37; N, 4.96.

4.3.11. 3-(4-Methoxyphenyl)-3-oxo-1-phenylpropyl diethylcarbamodithioate (2k)

^{1}H NMR (300 MHz, $CDCl_3$): δ 1.25–1.28 (m, 6H); 3.63–3.71 (m, 3H); 3.84 (s, 3H); 4.00–4.11 (m, 3H); 5.68–5.73 (dd, J = 4.4, 10.0 Hz, 1H); 6.87–6.92 (m, 2H); 7.18–7.43 (m, 5H); 7.94–8.06

(m, 2H). ESI-MS: 388.1 ($C_{21}H_{26}NO_2S_2$, $[M+H]^+$). Anal. Calcd for $C_{21}H_{25}NO_2S_2$: C, 65.08; H, 6.50; N, 3.61. Found: C, 65.41; H, 6.78; N, 3.98.

4.3.12. 3-(4-Bromophenyl)-3-oxo-1-phenylpropyl diethylcarbamodithioate (2l)

^{1}H NMR (300 MHz, $CDCl_3$): δ 1.22–1.29 (m, 6H); 3.62–4.15 (m, 6H); 5.62–5.67 (dd, J = 4.4, 10.3 Hz, 1H); 7.19–7.31 (m, 3H); 7.37–7.45 (m, 2H); 7.54–7.59 (m, 2H); 7.77–7.90 (m, 2H). ESI-MS: 436.0 ($C_{20}H_{23}BrNOS_2$, $[M+H]^+$). Anal. Calcd for $C_{20}H_{22}BrNOS_2$: C, 55.04; H, 5.08; N, 3.21. Found: C, 55.35; H, 5.32; N, 3.54.

4.3.13. 3-(3,4-Dichlorophenyl)-3-oxo-1-phenylpropyl diethylcarbamodithioate (2m)

^{1}H NMR (300 MHz, $CDCl_3$): δ 1.25–1.32 (m, 6H); 3.60–4.05 (m, 6H); 5.59–5.65 (dd, J = 4.4, 10.4 Hz, 1H); 7.20–8.10 (m, 8H). ESI-MS: 425.0 ($C_{20}H_{22}Cl_2NOS_2$, $[M+H]^+$). Anal. Calcd for $C_{20}H_{21}Cl_2NOS_2$: C, 56.33; H, 4.96; N, 3.28. Found: C, 56.79; H, 5.25; N, 3.44.

4.3.14. 3-(4-Chlorophenyl)-3-oxo-1-phenylpropyl diethylcarbamodithioate (2n)

^{1}H NMR (300 MHz, $CDCl_3$): δ 1.24–1.28 (m, 6H); 2.97–4.01 (m, 6H); 5.63–5.68 (dd, J = 4.4, 10.2 Hz, 1H); 7.19–7.98 (m, 9H). ESI-MS: 392.1 ($C_{20}H_{23}ClNOS_2$, $[M+H]^+$). Anal. Calcd for $C_{20}H_{22}ClNOS_2$: C, 61.28; H, 5.66; N, 3.56. Found: C, 61.54; H, 5.87; N, 3.87.

4.3.15. 3-(4-Bromophenyl)-1-(4-methoxyphenyl)-3-oxopropyl diethylcarbamodithioate (2o)

^{1}H NMR (300 MHz, $CDCl_3$): δ 1.22–1.27 (m, 6H); 3.51–3.73 (m, 3H); 3.75 (s, 3H); 3.85–4.02 (m, 3H); 5.56–5.61 (dd, J = 4.4, 10.6 Hz, 1H); 6.77–6.83 (m, 1H); 7.25–7.32 (m, 1H); 7.53–7.89 (m, 6H). ESI-MS: 466.0 ($C_{21}H_{25}BrNO_2S_2$, $[M+H]^+$). Anal. Calcd for $C_{21}H_{24}BrNO_2S_2$: C, 54.07; H, 5.19; N, 3.00. Found: C, 54.38; H, 5.28; N, 3.17.

4.3.16. 3-(4-Bromophenyl)-1-(4-fluorophenyl)-3-oxopropyl diethylcarbamodithioate (2p)

^{1}H NMR (300 MHz, $CDCl_3$): δ 1.25–1.32 (m, 6H); 3.66–4.07 (m, 6H); 5.62–5.67 (dd, J = 4.2, 10.3 Hz, 1H); 6.94–6.99 (m, 2H); 7.35–7.39 (m, 2H); 7.56–7.66 (m, 2H); 7.82–7.85 (m, 2H). ESI-MS: 454.0 ($C_{20}H_{22}BrFNOS_2$, $[M+H]^+$). Anal. Calcd for $C_{20}H_{21}BrFNOS_2$: C, 52.86; H, 4.66; N, 3.08. Found: C, 52.97; H, 4.73; N, 3.31.

4.3.17. 1,3-Bis (4-methoxyphenyl) -3-oxopropyl diethylcarbamodithioate (2q)

^{1}H NMR (300 MHz, $CDCl_3$): δ 1.20–1.26 (m, 6H); 3.51–3.75 (m, 3H); 3.77 (s, 3H); 3.81 (s, 3H); 3.85–3.99 (m, 3H); 5.54–5.60 (dd, J = 4.4, 10.3 Hz, 1H); 6.78–6.89 (m, 4H); 7.25–7.82 (m, 4H). ESI-MS: 418.1 ($C_{22}H_{28}NO_3S_2$, $[M+H]^+$). Anal. Calcd for $C_{22}H_{27}NO_3S_2$: C, 63.28; H, 6.52; N, 3.35. Found: C, 63.53; H, 6.64; N, 3.57.

4.3.18. 3-(4-Methoxyphenyl)-3-oxo-1-*p*-tolylpropyl diethylcarbamodithioate (2r)

^{1}H NMR (300 MHz, $CDCl_3$): δ 1.12–1.25 (m, 6H); 2.39 (s, 3H); 3.60–3.68 (m, 2H); 3.84 (s, 3H); 3.88–4.02 (m, 4H); 5.62–5.67 (dd, J = 4.4, 10.3 Hz, 1H); 6.88–6.99 (m, 2H); 7.20–7.31 (m, 2H); 7.44–7.55 (m, 2H); 7.94–8.05 (m, 2H). ESI-MS: 402.1 ($C_{22}H_{28}NO_2S_2$, $[M+H]^+$). Anal. Calcd for $C_{22}H_{27}NO_2S_2$: C, 65.80; H, 6.78; N, 3.49. Found: C, 65.93; H, 6.86; N, 3.78.

4.3.19. 1-(2Chlorophenyl)-3-(4-methoxyphenyl)-3-oxopropyl diethylcarbamodithioate (2s)

^{1}H NMR (300 MHz, $CDCl_3$): δ 1.24–1.32 (m, 6H); 3.69–4.07 (m, 6H); 3.84 (s, 3H); 6.07–6.12 (dd, J = 4.9, 9.7 Hz, 1H); 6.82–6.97 (m, 2H); 7.13–7.20 (m, 2H); 7.30–7.52 (m, 2H); 7.97–8.05 (m, 2H). ESI-MS: 422.1 ($C_{21}H_{25}ClNO_2S_2$, $[M+H]^+$). Anal. Calcd for $C_{21}H_{24}ClNO_2S_2$: C, 59.77; H, 5.73; N, 3.32. Found: C, 59.95; H, 5.92; N, 3.51.

4.3.20. 1-(4-Chlorophenyl)-3-(4-methoxyphenyl)-3-oxopropyl diethylcarbamodithioate (2t)

^{1}H NMR (300 MHz, $CDCl_3$): δ 1.23–1.27 (m, 6H); 3.63–3.70 (m, 2H); 3.85 (s, 3H); 3.88–4.05 (m, 4H); 5.67–5.72 (dd, J = 4.4, 10.1 Hz, 1H); 6.87–6.91 (m, 2H); 7.32–7.58 (m, 4H); 7.92–7.97 (m, 2H). ESI-MS: 422.1 ($C_{21}H_{25}ClNO_2S_2$, $[M+H]^+$). Anal. Calcd for $C_{21}H_{24}ClNO_2S_2$: C, 59.77; H, 5.73; N, 3.32. Found: C, 59.97; H, 5.94; N, 3.52.

4.4. Crystal structure determination

Crystal structure determination of compound **2l** were carried out on a Nonius CAD4 diffractometer equipped with graphite-monochromated Mo Kα (λ = 0.71073 Å) radiation. The structure was solved by direct methods and refined on F^2 by full-matrix least-squares methods using SHELX-97.[32] All the non-hydrogen atoms were refined anisotropically. All the hydrogen atoms were placed in calculated positions and were assigned fixed isotropic thermal parameters at 1.2 times the equivalent isotropic U of the atoms to which they are attached and allowed to ride on their respective parent atoms. The contributions of these hydrogen atoms were included in the structure-factors calculations. The crystal data, data collection, and refinement parameter for the compound **2l** is listed in Table 3.

4.5. Anti-proliferation assay

The antiproliferative activity of the prepared compounds against MCF-7 human breast carcinoma cells was evaluated as described elsewhere[11] with some modifications. Target tumor cell line was grown to log phase in RPMI 1640 medium supplemented with 10% fetal bovine serum. After diluting to 2×10^4 cells mL^{-1} with the complete medium, 100 μL of the obtained cell suspension was added to each well of 96-well culture plates. The subsequent incubation was permitted at 37 °C, 5% CO_2 atmosphere for 24 h before the cytotoxicity assessments. Tested samples at pre-set concentrations were added to 6 wells with colchicine and CSA-4 co-assayed as positive reference. After 48 h exposure period, 40 μL of PBS containing 2.5 mg mL^{-1} of MTT (3-(4,5-dimethylthiazol-2-yl)-2,5-diphenyltetrazolium bromide)) was added to each well.

Table 3
Crystallographical and experimental data for compound **2l**

Compounds	**2l**
Empirical formula	$C_{20}H_{22}BrNOS_2$
Formula weight	436.42
Crystal system	Monoclinic
Space group	$P2(1)/n$
a (Å)	7.5824(6)
b (Å)	15.8153(14)
c (Å)	16.9183(15)
α (°)	90.00
β (°)	94.548(4)
γ (°)	90.00
V (Å)	2022.4(3)
Z	4
D_{calcd}/g cm^{-3}	1.433
θ range (°)	2.42–25.00
F(0 0 0)	896
Reflections collected/unique	10,445/3549 [R_{int} = 0.0287]
Data/restraints/parameters	3549/0/228
Absorption coefficient (mm^{-1})	2.247
R_1; wR_2 [$I > 2\sigma(I)$]	0.0315/0.0636
R_1; wR_2 (all data)	0.0531/0.0709
GOF	1.020

4 h later, 100 μL extraction solution (10% SDS–5% isobutyl alcohol–0.01 M HCl) was added. After an overnight incubation at 37 °C, the optical density was measured at a wavelength of 570 nm on an ELISA microplate reader. In all experiments three replicate wells were used for each drug concentration. Each assay was carried out at least three times. The results were summarized in Table 2.

4.6. Effects on tubulin polymerization

Bovine brain tubulin was purified as described previously.[33] To evaluate the effect of the compounds on tubulin assembly in vitro,[34] varying concentrations were preincubated with 10 μM tubulin in glutamate buffer at 30 °C and then cooled to 0 °C. After addition of GTP, the mixtures were transferred to 0 °C cuvettes in a recording spectrophotometer and warmed-up to 30 °C and the assembly of tubulin was observed turbidimetrically. The IC_{50} was defined as the compound concentration that inhibited the extent of assembly by 50% after 20 min incubation.

4.7. Docking simulations

Molecular docking of compound **2n** into the three-dimensional X-ray structure of tubulin (PDB code: 1SA0) was carried out using the Auto-Dock software package (version 4.0) as implemented through the graphical user interface Auto-Dock Tool Kit (ADT 1.4.6).[28,35]

The graphical user interface ADT was employed to set up the enzymes: all hydrogens were added, Gasteiger charges were calculated and nonpolar hydrogens were merged to carbon atoms. For macromolecules, generated pdbqt files were saved.

The 3D structure of ligand molecule was built, optimized (PM3) level, and saved in Mol2 format with the aid of the molecular modeling program SPARTAN (Wavefunction Inc.). These partial charges of Mol2 file was further modified by using the ADT package (vision 1.4.6) so that the charges of the nonpolar hydrogens atoms assigned to the atom to which the hydrogen is attached. The resulting file was saved as pdbqt file.

AutoDock 4.0 was employed for all docking calculations. The ADT program was used to generate the docking input files. A grid box size of $44 \times 46 \times 42$ points in *x*, *y* and *z* directions was built and the grid center located in (116.909, 89.688, 7.094) in the catalytic site of the protein. A grid spacing of 0.375 Å (approximately one forth of the length of carbon–carbon covalent bond) and a distance-dependent function of the dielectric constant were used for the calculation of the energetic map. Ten runs were generated by using Lamarckian genetic algorithm searches. Default setting was used with an initial population of 50 randomly placed individuals, a maximum number of 2.5×10^6 energy evaluations, and a maximum number of 2.7×10^4 generations. A mutation rate of 0.02 and a crossover rate of 0.8 were chosen. Results differing by less than 0.5 Å in positional root-mean-square deviation (RMSD) were clustered together and the results of the most favorable free energy of binding were selected as the resultant complex structures.

5. Supplementary data

Crystallographic data for the structural analysis have been deposited with the Cambridge Crystallographic Data Centre Nos. 750890 for **2l**. A copy of this information can be obtained free of charge from The Director, CCDC, 12 Union Road, Cambridge CB2 1EZ, UK (fax: +44 1223 336 033; e-mail: deposit@ccdc.cam.ac.uk or www: http://www.ccdc.cam.ac.uk).

Acknowledgement

This work was supported by the Jiangsu National Science Foundation (No. BK2009239) and by a grant (Project 30772627) from National Natural Science Foundation of China.

References and notes

1. Valiron, O.; Caudron, N.; Job, D. *Cell. Mol. Life Sci.* **2001**, *58*, 2069.
2. Hamel, E. *Med. Chem. Rev.* **1996**, *16*, 207.
3. Kim, D. Y.; Kim, K. H.; Kim, N. D.; Lee, K. Y.; Han, C. K.; Yoon, J. H.; Moon, S. K.; Lee, S. S.; Seong, B. L. *J. Med. Chem.* **2006**, *49*, 5664.
4. Chinigo, G. M.; Paige, M.; Grindrod, S.; Hamel, E.; Dakshamamurthy, S.; Chruszcz, M.; Minor, W.; Brown, M. L. *J. Med. Chem.* **2008**, *51*, 4620.
5. Romagnoli, R.; Baraldi, P. G.; Carrion, M. D.; Cruz-Lopez, O.; Cara, C. L.; Basso, G.; Viola, G.; Khedr, M.; Balzarini, J.; Mahboobi, S.; Sellmer, A.; Brancale, A.; Hamel, E. *J. Med. Chem.* **2009**, *52*, 5551.
6. Pettit, G. R.; Singh, S. B.; Hamel, E.; Lin, C. M.; Alberts, D. S.; Garcia-Kendall, D. *Experentia* **1989**, *45*, 209.
7. Lin, C. M.; Ho, H. H.; Pettit, G. R.; Hamel, E. *Biochemistry* **1989**, *28*, 6984.
8. Ravelli, R. B.; Gigant, B.; Curmi, P. A.; Jourdain, I.; Lachkar, S.; Sobel, A.; Knossow, M. *Nature* **2004**, *428*, 198.
9. Lawrence, N. J.; McGown, A. T. *Curr. Pharm. Des.* **2005**, *11*, 1679.
10. Nowakowska, Z. *Eur. J. Med. Chem.* **2007**, *42*, 125.
11. Boumendjel, A.; Boccard, J.; Carrupt, P.-A.; Nicolle, E.; Blanc, M.; Geze, A.; Choisnard, L.; Wouessidjewe, D.; Matera, E.-L.; Dumontet, C. *J. Med. Chem.* **2008**, *51*, 2307.
12. Cabrera, M.; Simoens, M.; Falchi, G.; Lavaggi, M. L.; Piro, O. E.; Castellano, E. E.; Vidal, A.; Azqueta, A.; Monge, A.; Lopez de Cerain, A.; Sagrera, G.; Seoane, G.; Cerecetto, H.; Gonzalez, M. *Bioorg. Med. Chem.* **2007**, *15*, 3356.
13. Sabzevari, O.; Galati, G.; Moridani, M. Y.; Siraki, A.; O'Brien, P. J. *Chem. Biol. Interact.* **2004**, *148*, 57.
14. Rao, Y. K.; Fang, S.-H.; Tzeng, Y.-M. *Bioorg. Med. Chem.* **2004**, *12*, 2679.
15. Liu, M.; Wilairat, P.; Croft, S. L.; Tan, A. L.-C.; Go, M.-L. *Bioorg. Med. Chem.* **2003**, *11*, 2729.
16. Lunardi, F.; Guzela, M.; Rodriguez, A. T.; Correa, R.; Eger-Mangrich, I.; Steindel, M.; Grisard, E. C.; Assreuy, J.; Calixto, J. B.; Santos, A. R. S. *Antimicrob. Agents Chemother.* **2003**, *47*, 1449.
17. Go, M. L.; Wu, X.; Liu, X. L. *Curr. Med. Chem.* **2005**, *12*, 483.
18. Kerr, D. J.; Hamel, E.; Jung, M. K.; Flynn, B. L. *Bioorg. Med. Chem.* **2007**, *15*, 3290.
19. Jung, J. C.; Jang, S.; Lee, Y.; Min, D.; Lim, E.; Jung, H.; Miyeon, Oh.; Seikwan, Oh.; Jung, M. *J. Med. Chem.* **2008**, *51*, 4054.
20. Cvek, B.; Dvorak, Z. T. *Curr. Pharm. Des.* **2007**, *30*, 3155.
21. Safak, C.; Erdogan, H.; Ertan, M.; Yulug, N. *J. Chem. Soc. Rak.* **1990**, *12*, 296.
22. Aragonés, J.; López-Rodríguez, C.; Corbi, A.; Gómez del Arco, P.; López-Cabrera, M.; Landazuri, M.; Redondo, J. M. *J. Biol. Chem.* **1996**, *271*, 10924.
23. Xie, J.; Funakoshi, T.; Shimada, H.; Kojima, S. *J. Appl. Toxicol.* **1997**, *16*, 317.
24. Funakoshi, T.; Ueda, K.; Shimada, H.; Kojima, S. *Toxicology* **1997**, *116*, 99.
25. Tandon, S. K.; Singh, S.; Prasad, S. *Hum. Exp. Toxicol.* **1997**, *16*, 557.
26. Huang, W.; Ding, Y.; Miao, Y.; Liu, M. Z.; Li, Y.; Yang, G. F. *Eur. J. Med. Chem.* **2009**, *44*, 3687.
27. Azizi, N.; Ebrahimi, F.; Aakbari, E.; Aryanasab, F. R.; Saidi, M. *Synlett* **2007**, 2797.
28. Huey, R.; Morris, G. M.; Olson, A. J.; Goodsell, D. S. *J. Comput. Chem.* **2007**, *28*, 1145.
29. De Martino, G.; Edler, M. C.; La Regina, G.; Coluccia, A.; Barbera, M. C.; Barrow, D.; Nicholson, R. I.; Chiosis, G.; Brancale, A.; Hamel, E.; Artico, M.; Silvestri, R. *J. Med. Chem.* **2006**, *49*, 947.
30. Zhang, Q.; Peng, Y. Y.; Wang, X. I.; Keenan, S. M.; Arora, S.; Welsh, W. J. *J. Med. Chem.* **2007**, *50*, 749.
31. Chiang, Y. K.; Kuo, C. C.; Wu, Y. S.; Chen, C. T.; Coumar, M. S.; Wu, J. S.; Hsieh, H. P.; Chang, C. Y.; Jseng, H. Y.; Wu, M. H.; Leou, J. S.; Song, J. S.; Chang, J. Y.; Lyu, P. C.; Chao, Y. S.; Wu, S. Y. *J. Med. Chem.* **2009**, *52*, 4221.
32. Sheldrick, G. M. SHELX-97. *Program for X-ray Crystal Structure Solution and Refinement*, Göttingen University, Germany, 1997.
33. Hamel, E.; Lin, C. M. *Biochemistry* **1984**, *23*, 4173.
34. Hamel, E. *Cell Biochem. Biophys.* **2003**, *38*, 1.
35. Morris, G. M.; Goodsell, D. S.; Halliday, R. S.; Huey, R.; Hart, W. E.; Belew, R. K.; Olson, A. J. *J. Comput. Chem.* **1998**, *19*, 1639.